Mitigation of Acoustic Resonance using Electrically Shunted Loudspeakers

Andrew J. Fleming[a], Dominik Niederberger[b], S. O. Reza Moheimani[a] and Manfred Morari[b]

[a]School of Electrical Engineering and Computer Science, University of Newcastle, Australia;
[b]Automatic Control Laboratory, Swiss Federal Institute of Technology, Switzerland.

ABSTRACT

Low-frequency reverberant sound fields are usually suppressed by means of either adaptive feedforward control or Helmholtz resonator. In this paper, an electrical impedance is connected to the terminals of an acoustic loudspeaker, the mechanical dynamics, and hence acoustic response can be made to emulate a sealed acoustic resonator. No microphone or velocity measurement is required. In some cases, the required electrical circuit is simply the parallel connection of a capacitor and resistor. Experimental application to a closed acoustic duct results in 14 dB pressure attenuation of a single acoustic mode.

Keywords: Resonant, Acoustic, Electrical Shunt, Loud Speaker, Damping

1. INTRODUCTION

Since the original work of Leug [1], and Olson and May [2], the problem of low-frequency acoustic noise attenuation has been studied throughout the industrial and academic domains. High-frequency acoustic noise (greater than 500Hz) is generally addressed with a combination of porous damping materials [3], Helmholtz resonators [4] [5], and mufflers [5]. Unfortunately such technologies do not offer acceptable absorbance at lower frequencies. Porous damping materials rely on the viscous damping of fluid flow over a surface. As particle velocity is proportional to frequency, impractical volumes of material are required at frequencies below 500Hz. Helmholtz resonators, the acoustic equivalent of a mechanical tuned-mass absorber, provide excellent attenuation of highly resonant acoustic modes but require restrictively large cavity volumes at frequencies below 200 Hz. The inadequacy of traditional passive damping treatments has motivated a diverse literature on the active control of low-frequency reverberant noise.

The field of non-traditional acoustic noise control can be grouped roughly into 5 categories: 1) Passive baffles and compliant panels [6–9], 2) Helmholtz resonators [4, 10–13], 3) Feedforward noise control [14–18], 4) Feedback noise control [2, 19–22], and 5) Impedance Based [23–27]. None of these techniques simultansously contain all of the desireable characteristics: low weight, volume, and power requirements; low complexity; simple design and tuning; high performance with low sensitivity to environmental variations.

In this paper we present a new technique for the attenuation of reverberant sound fields. The goal is to globally reduce acoustic response without the need for either a precise plant model, collocated pressure sensor, or constant volume velocity source. By identifying the interaction between sound-field, mechanical speaker, and electromagnetic transducer, a simple electrical impedance can be designed, that when connected to a speaker coil, improves the dissipation of acoustic energy. The designed electrical impedance that effectively renders the speaker as an acoustic resonator does not require a model for design and can be tuned experimentally or adaptively. Under certain circumstances, the electrical impedance can be simplified to a passive resistor and capacitor.

In Section 2, the electro-mechanical-acoustic coupling is described. An electrical equivalent model is also presented that facilitates intuitive impedance design. In Section 3, impedance designs are applied to an experimental duct system. The paper is concluded in Section 4.

E-mail: andrew.fleming@newcastle.edu.au

Smart Structures and Materials 2006: Damping and Isolation, edited by William W. Clark, Mehdi Ahmadian, Arnold Lumsdaine, Proc. of SPIE Vol. 6169, 616918, (2006) · 0277-786X/06/$15 · doi: 10.1117/12.659022

Figure 1. Experimental duct with two transversely mounted loudspeakers

2. SYSTEM DYNAMICS

The majority of techniques for acoustic noise control are targeted at a specific problem scenario. In this work, our objective is to reduce pressure variation within a sealed duct in response to a planar velocity disturbance. The experimental apparatus, comprising a PVC pipe, with two transversely mounted speaker ports is shown in Figure 1. Dimensions and the location of pressure, velocity, and electrical measurements can be found in Figure 2.

A velocity disturbance is introduced artificially using speaker 1. By exciting the speaker with a voltage, the applied velocity disturbance is measured directly using a Polytec Laser Vibrometer (PSV300). The two pressure measurements p_1 and p_2 are acquired using B&K 4935 array microphones with a Nexus preamplifier. While p_1 is used for performance evaluation, p_2 is required for analysis and control design purposes. The velocity of the control speaker, speaker 2, is also measured using the vibrometer. When the speaker is mounted onto the duct, the baffle velocity is measured through the rear air vent.

The experimental apparatus was chosen to represent a simple 1 dimensional reverberant noise control problem. Although the apparatus most closely resembles an air conditioning duct, multi-dimensional extension to reverberant room noise is possible. Another system closely resembling the experimental apparatus is a launch vehicle payload enclosure. End-mounted speakers have been used with acoustic impedance based techniques for the mitigation of acoustic pressure forces on sensitive payloads [27].

In the following subsections, a dynamic model of the duct system is derived progressively. We begin by considering an ideal acoustic system, i.e. a hard walled enclosure disturbed by a perfect velocity source. The passive mechanical dynamics of a control loudspeaker are then augmented to the ideal acoustic system. Finally, the electromagnetic model is also included to relate the coil voltage and current, to the duct pressure and velocity. Many works in acoustic noise control simply neglect passive dynamics by modelling each loudspeaker as a velocity source. Although such works present analytic models, an extremely poor correspondence to experimental data is often observed. It is likely that a considerable portion of this disagreement can be attributed to unmodelled passive loudspeaker dynamics.

Other authors have also considered non-ideal acoustic systems, for example, systems with 'soft' walls, non-trivial end impedances [28], and passive speaker dynamics [28] [22]. In this work, the main objective is not to develop an exact model of the physical system, but rather to reveal the coupling and interaction between each domain. By illustrating the coupling in a graphical manner, simple impedance designs can be derived by inspection and experimental tuning.

2.1. Acoustic Dynamics

The governing equations relevant to the modelling of an acoustic enclosure are the fundamental equations of fluid mechanics: mass conservation, equation of state, and Euler's equation of motion. Linearization is possible in cases of small pressure perturbation and zero mean fluid velocity. The following wave equation for the acoustic

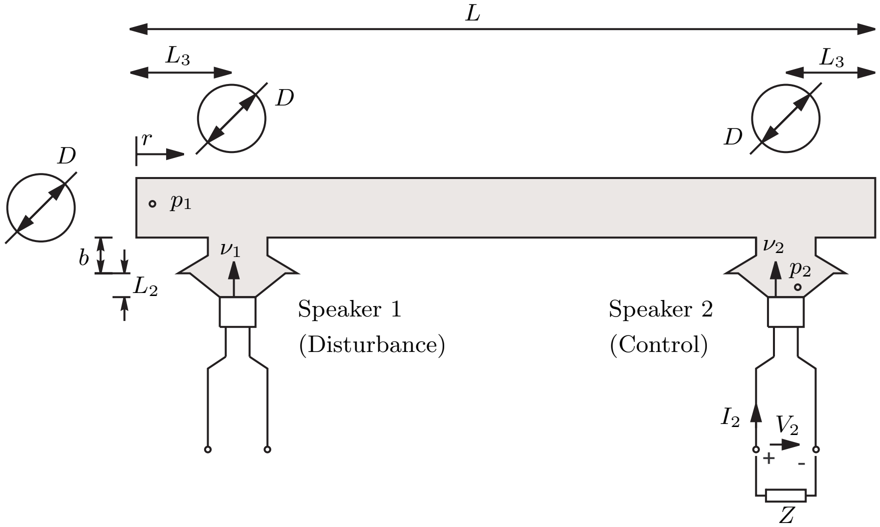

Parameter	length [mm]
D	150
b	150
L	4455
L_2	145
L_3	375

Figure 2. Acoustic duct geometry

duct shown in Figure 2 (without the control speaker 2) can be derived by combining the fundamental equations and solving for the fluid pressure [16],

$$\frac{\partial^2 p(r,t)}{\partial r^2} - \frac{1}{c^2}\frac{\partial^2 p(r,t)}{\partial t^2} = \rho_0 \frac{d\nu_1(t)}{dt}\delta(r - L_3) \tag{1}$$

subject to the closed-end boundary conditions

$$\nu(0,t) = \nu(L,t) = 0, \tag{2}$$

where $p(r,t)$ is the sound pressure variation measured r (meters) from the duct end, $\nu_1(t)$ is the forced velocity L_3 (meters) from the duct end, ρ_0 is the ambient density, and c is the speed of sound.

In the design and analysis of acoustic shunt impedances, the transfer function relating pressure to velocity at the control speaker baffle $G_{p_2\nu_2}(s)$ is of primary interest. A number of techniques are available in the literature for deriving closed-form solutions to (1). Examples considering side-mounted speakers can be found in references [29], [30] and [31].

The majority of practical acoustic systems contain properties difficult to model analytically, e.g. non-ideal boundary conditions, irregular geometries etc. It may be impossible to find a closed-form solution to the acoustic transfer function. In such cases, finite element analysis or system identification may present a viable alternative.

2.2. Including Loudspeaker Mechanical Dynamics

The equivalent mechanical diagram of an acoustic loudspeaker is illustrated in Figure 3 b). The mass, spring, and damping components correspond to the baffle weight, suspension stiffness, and suspension damping respectively. In this section, the unshunted system is considered, i.e. when $I_2 = 0$ which implies $F_{el} = 0$.

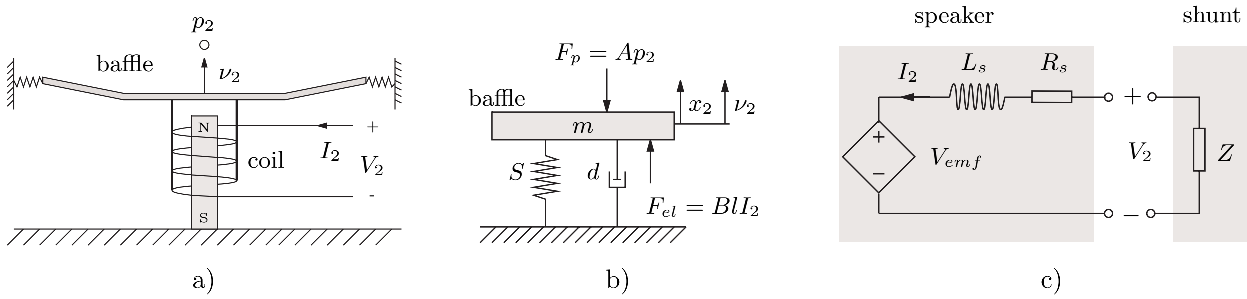

Figure 3. a) Sketch of the speaker, b) Mechanical equivalent diagram c) Electrical equivalent diagram

The response of the speaker can be expressed as a simple mass-spring-damper system

$$\ddot{x}_2 = \frac{1}{m}(-F_p - d\dot{x}_2 - Sx_2), \tag{3}$$

where x_2 denotes the inward baffle displacement, F_p is the acoustic force related to the pressure p_2, and m, S, and d are the equivalent mass, stiffness, and damping coefficients. In order to couple the loudspeaker and acoustic system, we require a transfer function $G_{\nu f}(s)$ relating the total applied force (in the direction opposite to F_p) to the baffle velocity ν_2. From equation (3), $G_{\nu f}(s)$ can be written in the frequency domain as,

$$G_{\nu f}(s) = \frac{\nu_2(s)}{-F_p(s)} = \frac{s}{s^2m + ds + S}. \tag{4}$$

By noting that the acoustic pressure develops a force proportional to the baffle surface area $F_p = Ap_2$, and that the resulting velocity ν_2 excites the acoustic system $G_{p_2\nu_2}(s)$, the two systems can be coupled. Figure 4 clearly illustrates the equivalence between a pressure feedback controller and the passive loudspeaker dynamics. The disturbance transfer function, measured from ν_1 to p_2 is modified from the open-loop response $G_{p_2\nu_1}(s)$ to,

$$\frac{p_2(s)}{\nu_1(s)} = \frac{G_{p_2\nu_1}(s)}{1 + C(s)G_{p_2\nu_2}(s)} \tag{5}$$

where the equivalent feedback controller $C(s)$ is

$$C(s) = G_{\nu f}(s)A. \tag{6}$$

Given that the loudspeaker acts to control the acoustic system, it is pertinent to identify and optimize the desirable characteristics during selection. The most obvious technique for increasing speaker influence is to increase the baffle area, as this directly affects the gain in the pressure feedback loop. The magnitude of the transfer function $G_{\nu f}(s)$ is also critical. Due to the gain roll-off of 20 dB per decade at frequencies greater than the mechanical cutoff, only low-frequency acoustic modes will be passively attenuated.

If a single dominant acoustic mode is the primary concern, a speaker with a lightly damped mechanical resonance, near in frequency, will achieve the greatest damping. The baffle resonance frequency can be altered by adding mass to the speaker cone. This should be done conservatively, as reducing the mechanical bandwidth of the speaker will also reduce the effective bandwidth over which the acoustic system can be controlled. Considering a single mode, if the frequency of mechanical and acoustic resonance is properly matched, the damping of the controller can be altered by shunting the coil with a resistor. As discussed fully in the following sections, if the inductive coil reactance is small, a resistive shunt will add mechanical damping.

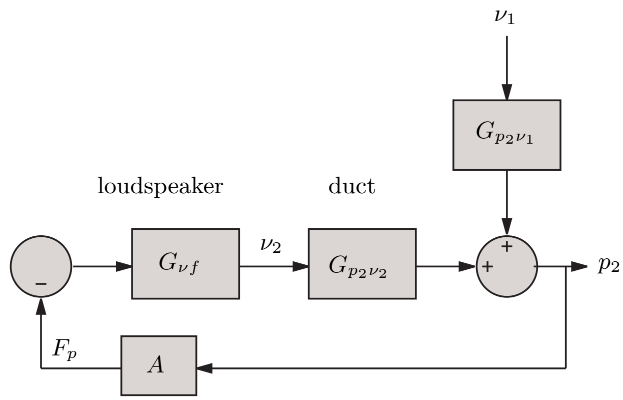

Figure 4. Block diagram of the composite acoustic and passive loudspeaker dynamics.

2.3. Including electromagnetic dynamics

As shown in Figure 3 c), the electromagnetic speaker dynamics can be modelled as a velocity dependent voltage source V_{emf}, in series with a resistor R_s, and inductor L_s. The induced voltage is related to the velocity by

$$V_{emf} = Bl\nu_2, \tag{7}$$

where B is the magnetic flux density, and l is the conductor length. If the speaker is short circuited, the orientation of the induced voltage, and hence induced current, hinders the application of an external velocity.

The force developed due to a current I_2 is equal to

$$F_{el} = BlI_2, \tag{8}$$

where F_{el} acts in the opposite direction to F_p and hence adds to the total force applied to the speaker, i.e.

$$\nu_2(s) = G_{\nu f}(s)(F_{el}(s) - F_p(s)). \tag{9}$$

If an electrical impedance $Z(s)$ is connected to the terminals of the speaker coil, the total voltage drop across the speaker impedance $sL_s + R_s$ is equal to the difference of the voltages across the speaker, V_2, and V_{emf}, i.e. the current flowing through the coil can be written as

$$I_2 = (V_2 - V_{emf})\frac{1}{sL_s + R_s}. \tag{10}$$

These relations are shown graphically in Figure 5. The electromagnetic dynamics introduce a further feedback loop around the velocity ν_2. In the special case where the loudspeaker is short-circuited, i.e. when $V_2 = 0$, and at frequencies below the cutoff of the filter $\frac{1}{sL_s+R_s}$, the coil acts as an electrodynamic brake. Physical damping is added to the mechanical speaker dynamics. Too much mechanical damping will reduce the acoustic performance of the speaker. A properly chosen resistance can be used to optimize the damping and passive acoustic mitigation.

Physical coupling between the electrical and acoustic domain is limited in each direction by the factor Bl. Good quality speakers with rare-earth magnets and dense, low-impedance windings will provide the best shunt circuit performance.

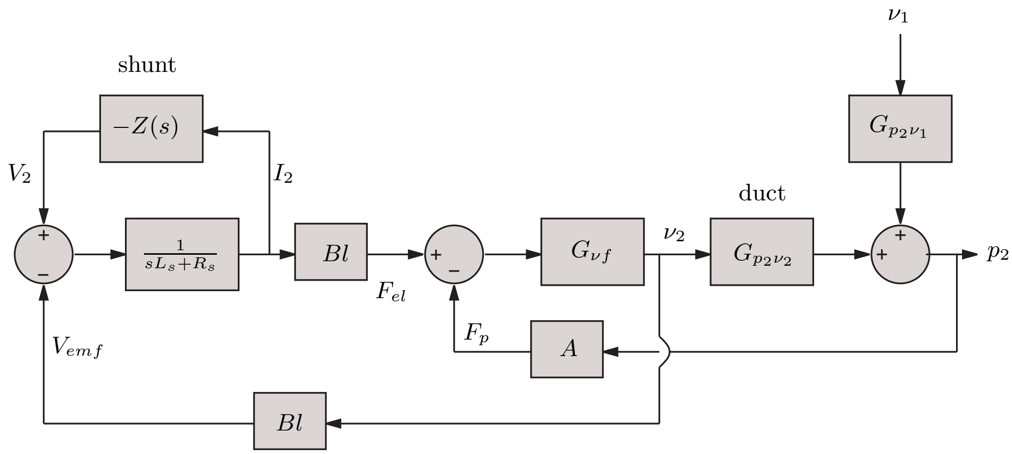

Figure 5. Block diagram of the composite acoustic, passive loudspeaker, and electromagnetic dynamics.

2.4. Helmholtz Resonators

Helmholtz resonators can reduce the response of undesirable acoustic modes by effecting a high absorption over a narrow frequency range. As shown in Figure 6a), a Helmholtz resonator comprises a cavity volume V coupled to the host sound field through a short tube of cross-section A and length l. In this figure, ν and p represent the air particle velocity and pressure at the resonator opening.

Due to the physical similarity to a lumped single-degree-of-freedom system, Helmholtz resonators can be equivalently represented as an electrical network. A diagrammatic representation of the equivalent acoustic, mechanical, and electrical systems can be found in Figure 6 a)-c), where c is the speed of sound, A the cross section, l the length of the tube, ρ the air density, and V the cavity volume. The stiffness $\frac{c^2\rho}{V}$ is a function of the enclosed air volume V, while the mass $\rho A(l + l_{corr}) = \rho A l_{eq}$ corresponds to the accelerated air in the tube, where l_{corr} is a correction factor accounting for additional air-mass at the tube opening. The correction factor is typically taken as $l_{corr} = 0.8R$, where R is the radius of the tube.

By inserting damping materials in the tube where air particle velocity is maximum, the damping d of the resonance can be increased. Note that the corresponding electrical parameters in Figure 6 c) are scaled by the factor $1/A^2$, this arises from the conversion $\tilde{p} = Ap$ and $\tilde{v} = Av$. The resonance frequency of the Helmholtz resonator without damping is [10]

$$\omega_{res} = c\sqrt{\frac{A}{V(l + l_{corr})}} = c\sqrt{\frac{A}{V l_{eq}}} = \frac{1}{\sqrt{L_{eq}C_{eq}}}, \tag{11}$$

where $L_{eq} = V/c^2\rho$, and $C_{eq} = \rho l_{eq}/A$.

2.5. Electrical Equivalent System

To aid in the understanding of the composite electrical, mechanical, and acoustic systems, as shown in Figure 5, it is helpful to cast each sub-system in the same physical domain. Given that our objective is to design a suitable shunt impedance, the choice of electrical domain permits a significant simplification of the complicated interactions shown in Figure 5.

The equivalent electrical network of the composite speaker-enclosure model is shown in Figure 7 a). The mechanical part of the speaker is modelled as a baffle mass m, a stiffness S and the mechanical damping d. The baffle is excited by the electrical force F_{el} proportional to the current I_2. The relationship $F_{el} = BlI_2$ is represented by a transformer. Analogously, the baffle acoustic force, $F_p = Ap_2$, is modelled by a gyrator.

In Figure 7a), only a single acoustic mode is considered, the volume air velocity at the baffle is denoted by $\nu_v = A\nu_2$.

The electrical part of the loudspeaker is modelled by the coil resistance R_s, inductance L_s, and induced voltage $V_{emf} = Bl\nu_2$.

By eliminating the gyrators and transformers using dual network elements and converting the values with A^2 and $(Bl)^2$ respectively, one obtains the simplified circuit shown in Figure 7 b). The corresponding mechanical part of the speaker performs like a Helmholtz resonator with resonance frequency $\omega_{res} = \sqrt{\hat{m}/\hat{S}}$ and damping $\hat{d}$. It is shown in the following, that these parameters can be modified through the application of a suitable electrical shunt impedance $Z(s)$.

3. PASSIVE SHUNT CIRCUIT DESIGN

In analogy to the field of piezoelectric shunt damping [32, 33], where an electrical circuit is shunted to the terminals of a piezoelectric transducer, a network connected to the terminals of a loudspeaker can be designed to moderate the response of a coupled acoustic enclosure. In this section, the design of passive shunt circuits is discussed.

Based on the electrical equivalent model introduced in Section 2.5, one observes that an enclosed speaker emulates the acoustic response of a Helmholtz resonator. If the properties of this *virtual* Helmholtz resonator can be adjusted, the speaker can be employed to attenuate a highly resonant acoustic mode in the same fashion as a physical Helmholtz resonator. In the following, shunt circuit topologies are presented that allow the parameters of the virtual Helmholtz resonator to be modified.

3.1. R Shunts

At low frequencies where $\omega \ll R_s/L_s$, the influence of the inductor L_s can be neglected. In this case, the Helmholtz damping $\hat{d}$ can be increased by connecting a resistor R to the terminals of the speaker. As observed in Figure 7 b), the resistor R in addition to the coil resistor R_s, appears in parallel to the mechanical damping $\hat{d}$. The total damping of the virtual Helmholtz resonator is then

$$\hat{d}_{tot} = \hat{d} + \frac{1}{R + R_s}. \tag{12}$$

Note that the total damping is restricted in range between $\hat{d}$ and $\hat{d} + 1/R_s$. A speaker with low $\hat{d}$ and R_s will provide the greatest tuning range.

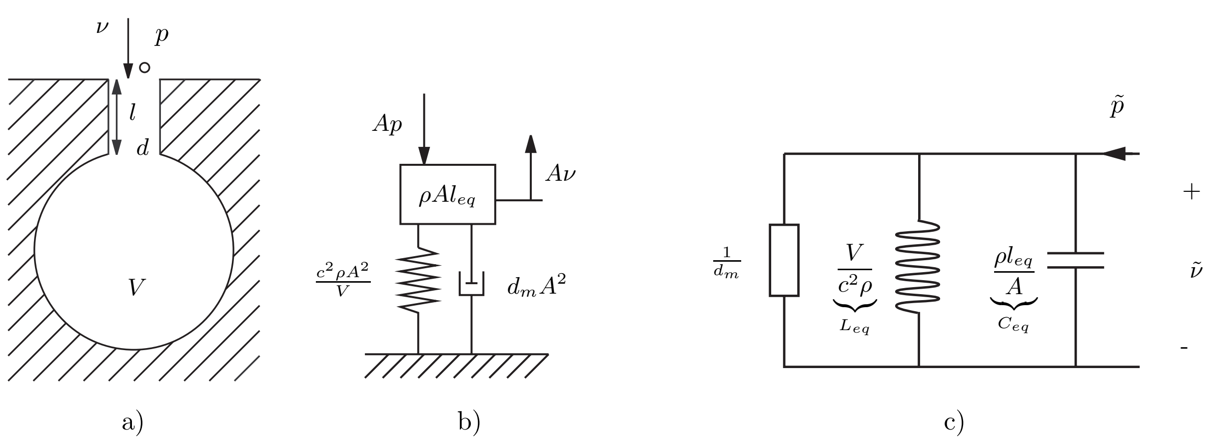

Figure 6. a) Sketch of the Helmholtz resonator, b) Equivalent mechanical model and c) equivalent electrical model.

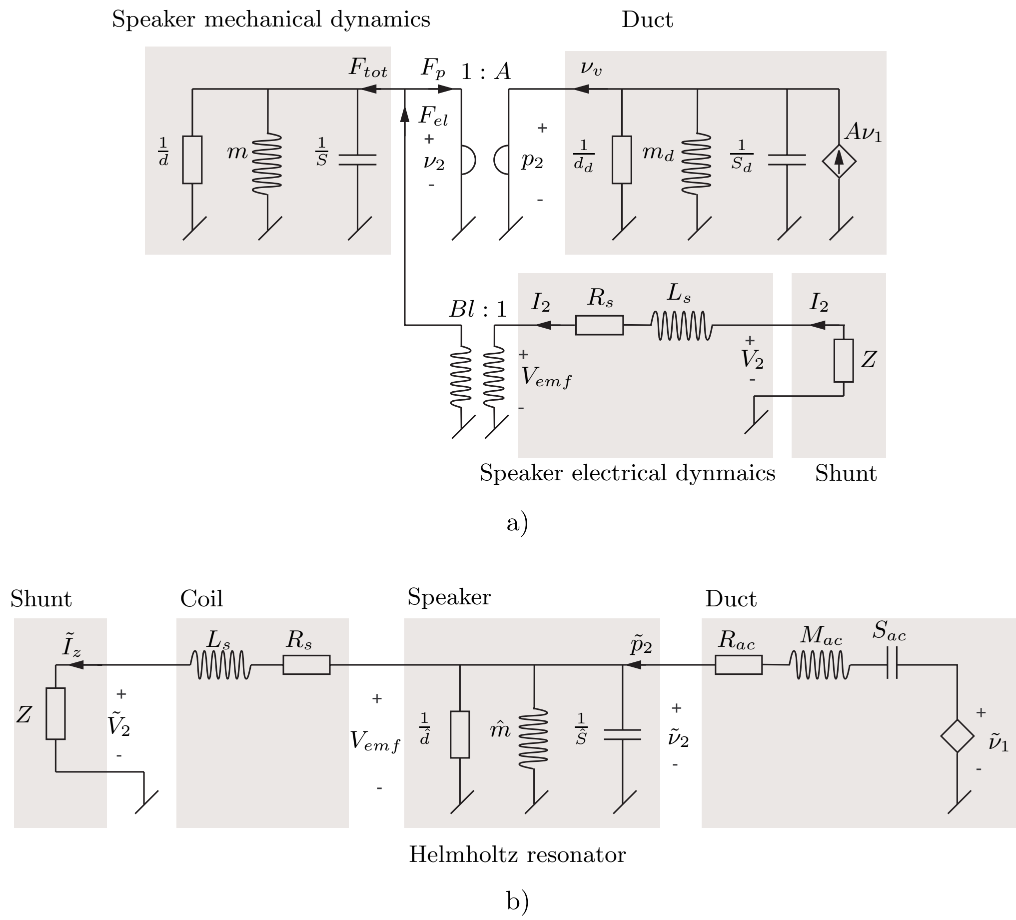

Figure 7. a) Electrical equivalent model of the composite speaker-enclosure system. b) simplified electrical equivalent.

The experimental application of a resistive shunt to the duct apparatus is shown in Figure 8a). For small values of R, the Helmholtz damping is large, thus, no influence on the duct system can be observed. For larger values of R, the resonator becomes more lightly damped until an anti-resonance appears at 40 Hz with new side-lobes at 30 and 50 Hz. As the Helmholtz frequency is improperly tuned, this system is not effective at suppressing noise.

3.2. $C//R$ Shunts

In the low frequency regime, i.e. where $\omega \ll R_s/L_s$, a parallel $C//R$ shunt circuit provides authority over the damping and resonance frequency of a virtual Helmholtz resonator. The addition of a parallel capacitor C_p effects an increase in the parameter $1/\hat{S}$. Thus, the Helmhotz resonance frequency can be reduced.

Experimental results from the application of a $C//R$ shunt circuit are shown in Figure 8 b). A capacitance and resistance of $C = 496\ \mu$F and $R_p = 8\ \Omega$ represents the correct adjustment of resonance frequency and damping. The properly tuned virtual Helmholtz resonator yields a first-mode attenuation of 11 dB. To the knowledge of the authors, a passive capacitor and resistor offers the best possible performance commensurate with simplicity and cost. It is important to note that only acoustic modes lower in frequency than both the mechanical and electrical speaker cutoff frequencies can be controlled. Thus, selection of a suitable speaker is critical to the performance of the system.

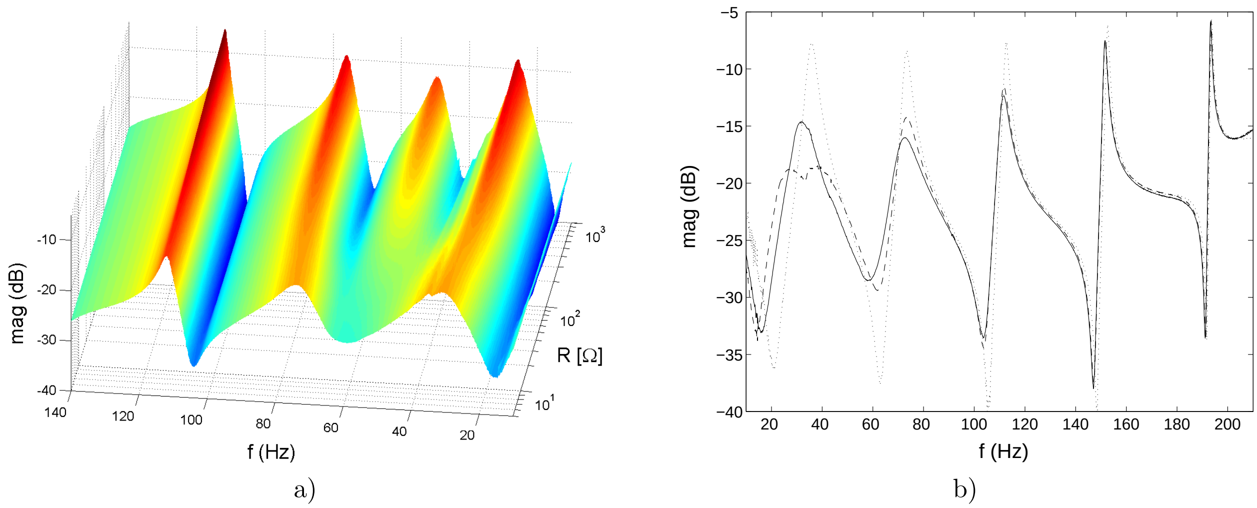

Figure 8. Measured magnitude of the transfer-function $G_{p_1 \nu_1}$. a) Passive R shunt b) Passive $R//C$ shunt. (...) duct without speaker, (—) duct with open speaker, (- -) duct with $C//R$ shunt tuned to the 1^{st} mode.

3.3. Negative $R - L$ with $R//L//C$ Shunts

By introducing a negative $R - L$ network as illustrated in Figure 9, a greater authority in the tuning ranges can be achieved. If the negative inductor and resistor are chosen equal, or close to the internal coil impedance, the electrical dynamics of the speaker can be essentially neglected. That is, $\tilde{R}_s = -R_s$ and $\tilde{L}_s = -L_s$, where $\tilde{R}_s$ and $\tilde{L}_s$ are estimates of the internal coil impedance.

With the use of an impedance cancelling network, an additional $R_p//L_p//C_p$ circuit, as shown in Figure 9 provides complete control over the virtual Helmholtz resonance frequency. As the capacitance C_p appears in parallel with $1/\hat{S}$, this parameter can be arbitrarily increased with an increase C_p. The other parameters are independent to variations in C_p, thus experimental tuning is straight-forward. A similar situation occurs with the relationship between L_p and $\hat{m}$. This parameter can be varied in either direction to increase or decrease the equivalent resonance frequency. Control over the damping parameter is restricted to values larger than d. The total damping is

$$\hat{d}_{tot} = \hat{d} + \frac{1}{R_p}. \tag{13}$$

Due to the requirement for negative network elements, practical implementation requires active circuit components. In the following experiments, a synthetic impedance [34, 35] is utilized to implement the shunt circuit impedance. An opamp based negative impedance converter is an alternative for the implementation of negative components.

Figure 10 demonstrates the experimental application of a negative $\tilde{R}_s - \tilde{L}_s$ and parallel $R_p//L_p//C_p$ for the attenuation of the first, second and third acoustic modes. The parameters of the shunt circuits are summarized in table 1. Compared to the duct with absent speaker, the acoustic response of each mode is suppressed by between 12 and 14 dB.

3.3.1. Improvement with serial L

One of the disadvantages associated with virtual Helmholtz resonators is the narrow-bandwidth of the control action. At resonance frequencies adjacent to that specifically controlled, the response of a lightly damping Helmholtz resonator can be likened to a hard wall, no absorption is provided. As shown in Figure 10 it may occur that high-frequency acoustic modes are actually enhanced when the speaker is tuned to damp a single

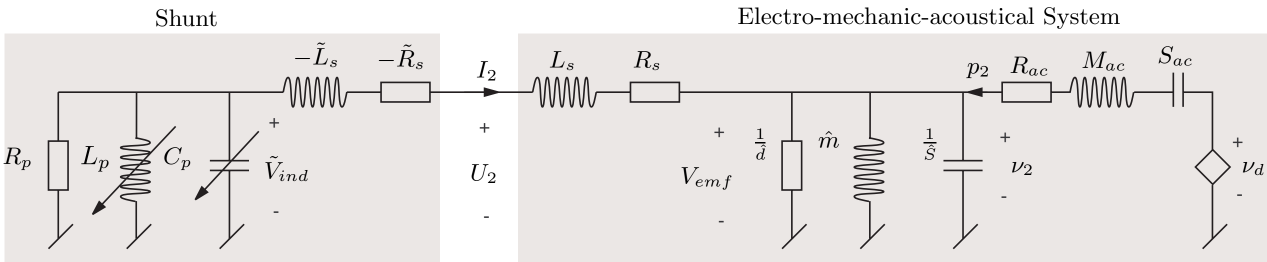

Figure 9. Shunt with negative $R_s - L_s$ and parallel $R//L//C$ network. All virtual Helmholtz parameters can be varied.

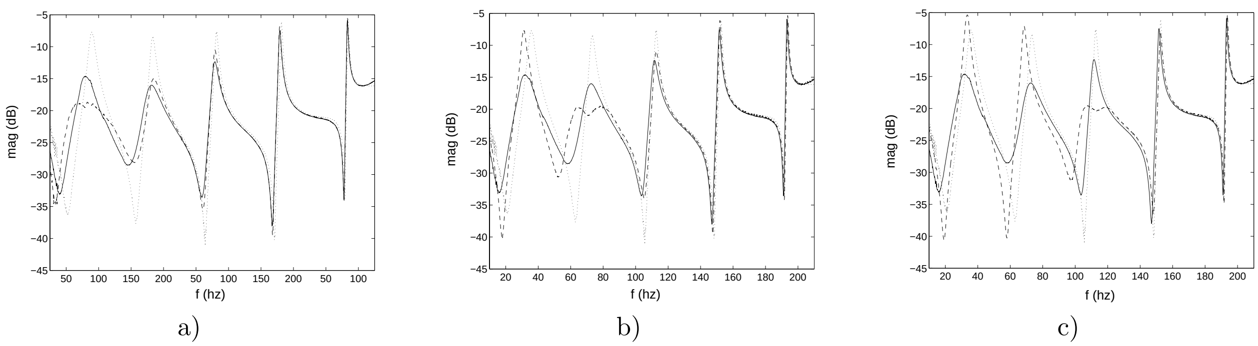

Figure 10. Negative $R_s - L_s$ with $R//L//C$ shunt. The shunt circuit is tuned to a) 1^{st} mode, b) 2^{nd} mode and c) 3^{rd} mode. (...) duct without speaker, (—) duct with open speaker, (- -) duct with shunt.

Mode	L_s [mH]	R_s [Ω]	R [Ω]	C [μF]	L [mH]	f [Hz]
1	-12	-12	23	116	> 1000	34
2	-12	-12	27	< 1	43.5	71
3	-12	-12	27	< 1	4.53	112

Table 1. Values for negative $R - L$ with $R//L//C$ shunts.

mode. This phenomenon can be attributed directly to the reduction of speaker bandwidth with the connection of shunt circuits described in the preceding sections.

The problem can be somewhat alleviated with the addition of a series inductor to the shunt circuit network. By increasing the electrical impedance at high frequencies, the braking behavior of the system can be reduced. As demonstrated in Figure 11, a series inductor can relax high-frequency speaker stiffening, and avoid unwanted enhancement of uncontrolled modes.

4. CONCLUSIONS

This paper extends the technique of passive shunt damping to acoustic loudspeakers.

By connecting an electrical impedance to the terminals of a loudspeaker, the mechanical dynamics of the loudspeaker are altered. Based on the mechanical and electrical properties of the loudspeaker, an electrical network can be designed that results in the loudspeaker emulating the acoustic response of a Helmholtz resonator. Highly resonant acoustic modes can be significantly attenuated. In some circumstances, depending on the frequency of resonance and the electromechanical properties of the loudspeaker, a passive capacitor and resistor can be employed to damp a single acoustic mode. Such simple and inherently stable impedances are useful in applications requiring high reliability and shock resistance, e.g. launch vehicle acoustic control. Experiments performed on a closed acoustic duct demonstrate the effectiveness of the proposed technique.

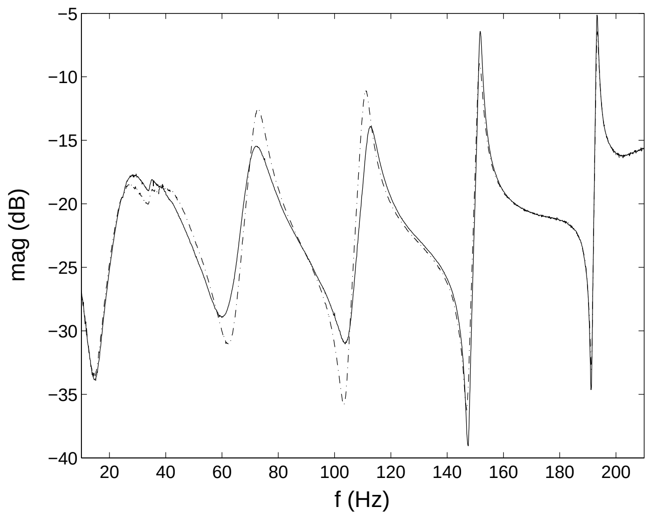

Figure 11. Measured magnitude of the transfer-function $G_{p_1\nu_1}$ using negative $\tilde{R}_s - \tilde{L}_s$ with $R_p//L_p//C_p$ and serial L shunt to improve damping of higher modes. (- -) negative $R-L$ with $R//L//C$ shunt, (—) improved shunt with additional series inductor.

REFERENCES

1. P. Leug, "Process of silencing sound oscillations," *U.S. Patent No. 2,043,416* , 1936.
2. H. F. Olsen and E. G. May, "Electronic sound absorber," *Journal of the Acoustical Society of America* **25**, pp. 1130–1136, 1953.
3. L. L. Beranek, *Noise and vibration control engineering: Principles and Applications*, Wiley-Interscience, New York, 1992.
4. U. Ingard, "On the theory and design of acoustic resonators," *Journal of the acoustical society of america* **20**, pp. 665–682, 1953.
5. M. L. Munjal, *Acoustics of ducts and mufflers*, Wiley-Interscience, New York, 1987.
6. A. Cummings, "The attenuation of sound in unlined ducts with flexible walls," *Journal of Sound and Vibration* **174**(4), pp. 433–450, 1994.
7. L. Huang, "A theory of reactive control of low-frequency duct noise," *Journal of Sound and Vibration* **238**(4), pp. 575–594, 2000.
8. R. D. Ford, "Panel sound absorbers," *Journal of Sound and Vibration* **10**(3), pp. 411–423, 1969.
9. W. Frommhold, H. V. Fuchs, and S. Sheng, "Acoustic performance of membrane absorbers," *Journal of Sound and Vibration* **170**(5), pp. 621–636, 1994.
10. R. Chanaud, "Effects of geometry on the resonance frequency of helmholtz resonators," *Journal of Sound and Vibration* **178**(3), pp. 337–348, 1994.
11. J. M. D. Bedout, M. A. Franchek, R. J. Bernhard, and L. Mongeau, "Adaptive passive noise control with self-tuning helmholtz resonators," *Journal of Sound and Vibration* **202**(1), pp. 109–123, 1997.
12. M. E. Johnson and S. Estève, "Comparison of local and global adaptive strategies for the control of broad-band noise in an enclosure using adaptive helmholtz resonantors," in *In Proc. Active 2002*, pp. 1111–1120, (Southhampton, UK), July 2002.
13. T. M. Kostek and M. A. Franchek, "Hybrid noise control in ducts," *Journal of Sound and Vibration* **237**(1), pp. 91–100, 2000.
14. K. Kido, "Reduction of noise by use of additional sound sources," in *In Proc. Inter-Noise '75*, pp. 647–650, (Sendai, Japan), 1975.
15. S. M. Kuo and D. R. Morgan, "Active noise control: A tutorial review," *Proceedings of the IEEE* **87**, pp. 943–973, June 1999.

16. P. A. Nelson and S. J. Elliott, *Active control of sound*, Academic Press, London, England, 1992.
17. C. P. Nowicki, D. P. Mendat, and D. G. Smith, "Active attenuation of motor/blower noise," in *In Proc. Noise-Con*, pp. 415–420, 1994.
18. U. Emborg, "Application of active noise control in saab 340 and saab 2000," in *In Proc. Nordic Conference on Vehicle and Machinery Vibrations*, (Stockholm, Sweden), September 1994.
19. R. L. Clark and D. G. Cole, "Active damping of enclosed sound fields through direct rate feedback control," *Journal of the Acoustical Society of America* **93**, pp. 1710–1716, March 1995.
20. S. A. Lane and R. L. Clark, "Dissipative feedback control of a reverberant enclosure using a constant volume velocity source," *ASME Journal of Vibration and Acoustics* **120**, pp. 987–993, October 1998.
21. S. A. Lane and R. L. Clark, "Improving loudspeaker performance for active noise control," *Journal of the Audio Engineering Society* **46**, pp. 508–519, June 1998.
22. R. L. Clark and K. D. Frampton, "Phase compensation for feedback control of enclosed sound fields," *Journal of Sound and Vibration* **195**(5), pp. 701–718, 1996.
23. D. Guicking and K. Karcher, "Active impedance control for one-dimensional sound," *ASME Journal of Vibration, Acoustics, Stress, and Reliability in Design* **106**, pp. 393–396, 1984.
24. D. Guicking and E. Lorentz, "An active sound absorber with porous plate," *ASME Journal of Vibration, Acoustics, Stress, and Reliability in Design* **106**, pp. 389–392, 1984.
25. J. P. Smith, B. D. Johnson, and R. A. Burdisso, "A broadband passive-active sound absorption system," *Journal of the Acoustical Society of America* **106**, pp. 2646–2652, November 1999.
26. T. Samejima, "A state feedback electro-acoustic transducer for active control of acoustic impedance," *Journal of the Acoustical Society of America* **113**(3), pp. 1483–1491, 2003.
27. J. D. Kemp and R. L. Clark, "Noise reduction in a launch vehicle fairing using actively tuned loudspeakers," *Journal of the Acoustical Society of America* **113**, pp. 1986–1994, April 2003.
28. B. J. Zimmer, S. P. Lipshitz, K. A. Morris, J. Vanderkooy, and E. E. Obasi, "An improved acoustic model for active noise control in a duct," *Transactions of the ASME* **125**, pp. 382–395, September 2003.
29. A. J. Hull, C. J. Radcliffe, and S. C. Southward, "Global active noise control of a one-dimensional acoustic duct using a feedback controller," *Transactions of the ASME* **115**, pp. 488–494, September 1993.
30. J. Hong, J. C. Akers, R. Venugopal, M. Lee, A. G. Sparks, P. D. Washabaugh, and D. Bernstein, "Modeling, identification, and feedback control of noise in an acoustic enclosure," *IEEE Transactions on Control Systems Technology* **4**, pp. 283–291, mAY 1996.
31. H. R. Pota and A. G. Kelkar, "Modeling and control of acoustic ducts," *Journal of Vibration and Acoustics* **123**, pp. 2–10, January 2001.
32. N. W. Hagood and A. Von Flotow, "Damping of structural vibrations with piezoelectric materials and passive electrical networks," *Journal of Sound and Vibration* **146**(2), pp. 243–268, 1991.
33. S. Moheimani, "A survey of recent innovations in vibration damping and control using shunted piezoelectric transducers," *IEEE Transactions on Control Systems Technology* **11**(4), pp. 482–494, 2003.
34. A. J. Fleming, S. Behrens, and S. O. R. Moheimani, "Synthetic impedance for implementation of piezoelectric shunt-damping circuits," *IEE Electronics Letters* **36**, pp. 1525–1526, August 2000.
35. A. Fleming and S. O. R. Moheimani, "Precision current and charge amplifiers for driving highly capacitive piezoelectric loads," *IEE Electronics Letters* **39**, pp. 282–294, February 2003.